

AD-A084 245

COLD REGIONS RESEARCH AND ENGINEERING LAB HANOVER NH  
DIFFERENCES BETWEEN EXPLOSIONS AND EARTHQUAKES, (U)  
MAR 80 C ZHICHEN, Z CHUANCHEN, H ZUOCHUN  
CRREL-TL-735

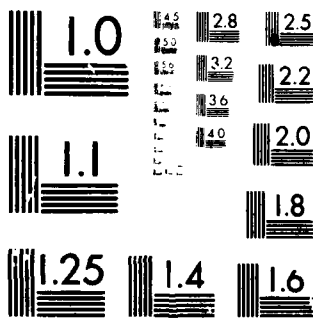
F/6 8/11

UNCLASSIFIED

NL

[ ]  
AD  
ACQUISITION

END  
DATE  
FILMED  
6-80  
DTIC



MICROCOPY RESOLUTION TEST CHART  
NATIONAL BUREAU OF STANDARDS-1963-A

Draft Translation 735

March 1980



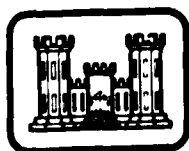
ADA 084245

# DIFFERENCES BETWEEN EXPLOSIONS AND EARTHQUAKES

Cheng Zhichen, Zhu Chuanchen, and Hu Zuochun

DTIC FILE COPY

DTIC  
ELECTE  
MAY 19 1980  
S D  
D



UNITED STATES ARMY  
CORPS OF ENGINEERS  
COLD REGIONS RESEARCH AND ENGINEERING LABORATORY  
HANOVER, NEW HAMPSHIRE, U.S.A.



Approved for public release; distribution unlimited

80 5 15 017

#### NOTICE

The contents of this publication have been translated as presented in the original text. No attempt has been made to verify the accuracy of any statement contained herein. This translation is published without copy editing or graphics preparation in order to expedite the dissemination of information. Requests for additional copies of this document should be addressed to the Defence Documentation Center, Cameron Station, Alexandria, Virginia 22314.

Unclassified

SECURITY CLASSIFICATION OF THIS PAGE (When Data Entered)

REPORT DOCUMENTATION PAGE		READ INSTRUCTIONS BEFORE COMPLETING FORM
1. REPORT NUMBER Draft Translation 735	2. GOVT ACCESSION NO. AD-A084245	3. RECIPIENT'S CATALOG NUMBER
4. TITLE (and Subtitle) DIFFERENCES BETWEEN EXPLOSIONS AND EARTHQUAKES	5. TYPE OF REPORT & PERIOD COVERED Translation	
6. PERFORMING ORG. REPORT NUMBER		7. AUTHOR(s) Cheng Zhichen, Zhu/Chuanchen, Hu/Zuochun
8. CONTRACT OR GRANT NUMBER(s)		9. PERFORMING ORGANIZATION NAME AND ADDRESS CRREL-TL-735
10. PROGRAM ELEMENT, PROJECT, TASK AREA & WORK UNIT NUMBERS		11. CONTROLLING OFFICE NAME AND ADDRESS U.S. Army Cold Regions Research and Engineering Laboratory Hanover, New Hampshire 03755
12. REPORT DATE Mar 80		13. NUMBER OF PAGES 23
14. MONITORING AGENCY NAME & ADDRESS (if different from Controlling Office)		15. SECURITY CLASS. (of this report) Unclassified
15a. DECLASSIFICATION/DOWNGRADING SCHEDULE		16. DISTRIBUTION STATEMENT (of this Report) Approved for public release; distribution unlimited.
17. DISTRIBUTION STATEMENT (of the abstract entered in Block 20, if different from Report) 21 Draft trans. of Acta Geophysica Sinica (China) v 18/n 3 p 208-216 Jul 75, by		
18. SUPPLEMENTARY NOTES Translator: Donald G. Albert, USACRREL		
19. KEY WORDS (Continue on reverse side if necessary and identify by block number) Earthquakes Explosions Seismic detection Seismic signatures Seismic waves		
20. ABSTRACT (Continue on reverse side if necessary and identify by block number) This paper investigates the differences between seismograms of industrial explosions and earthquakes of medium strength ( $2.5 < M_L < 4.5$ ) and at medium distances (100-500 km) in order to offer methods of distinguishing explosions from the records.		

Table of Contents

	<u>Page</u>
<b>List of Symbols</b>	
<b>Abstract</b> . . . . .	1
<b>I. Introduction</b> . . . . .	1
<b>II. Statistical differences between explosion and earthquake records</b> . . . . .	2
1. The relationship between $t_{\bar{P}-P_n}$ and $t_{\bar{S}-\bar{P}}$ . . . . .	2
2. The relationship between $M_L$ and $M_S$ . . . . .	4
3. The $S_V/S_H$ . . . . .	4
4. The ratio of $A_p/A_s$ . . . . .	6
5. Average period, $T$ , of the S waves. . . . .	7
6. S wave decay time $\tau$ . . . . .	8
7. Polarity distribution of primary ground motion . . . . .	9
8. Surface waves. . . . .	9
<b>III. Discussion</b> . . . . .	10
<b>References</b> . . . . .	11
<b>Figure Captions</b> . . . . .	12
<b>Figures</b> . . . . .	14

<b>Accession For</b>	
NTIS GRA&I	<input checked="" type="checkbox"/>
DDC TAB	<input type="checkbox"/>
Unannounced	<input type="checkbox"/>
Justification	<input type="checkbox"/>
<b>By</b> _____	
<b>Distribution/</b> _____	
<b>Availability Codes</b>	
<b>Dist.</b>	<b>Avail and/or special</b>
A	

**DTIC**  
**ELECTE**  
**S**      **D**  
 MAY 19 1980  
**D**

List of Symbols (added by the translator)

- $M_L$  - local magnitude  
 $M_S$  - surface wave magnitude  
 $m$  - body wave magnitude  
 $\bar{P}$  - direct compressional (P) wave  
 $P_n$  - refracted P wave  
 $P_L$  - long period P wave  
 $\bar{S}, S_L$  - direct and long period shear (S) waves  
 $S_H$  - horizontally polarized shear wave  
 $S_V$  - vertically polarized shear wave  
 $\Delta$  - epicentral distance, km  
 $T$  - period of wave, s  
 $H$  - crustal thickness, km  
 $h$  - focal depth, km  
 $t_x$  - travel time from source to detector for an X - type wave, s  
 $V_1$  - average velocity of P wave in the earth's crust  
 $V_2$  - average velocity of P wave in the earth's mantle  
 $A_x$  - amplitude of a wave of the X type  
 $\tau$  - S wave decay time, s  $\tau = t(A_S = \max) - t(A_S = 1/2 \max)$   
 $n$  - number of data points  
 $\sigma$  - standard deviation  
 $\sigma_{r\psi}$  - stress in the r -  $\psi$  plane  
 $\mu$  - rigidity modulus  
 $\bar{U}$  - displacement vector with components (u,v,w) in the (r, $\psi$ ,z) directions  
 $\phi$  - scalar potential  
 $\bar{A}$  - vector potential  
 $a, b, a', b', \hat{a}, \hat{b}$  - constants

## DIFFERENCES BETWEEN EXPLOSIONS and EARTHQUAKES \*

### I. Introduction

Along with the rapid progress of socialist reconstruction in China has come an increasing use of explosives in normal daily industrial mining. Therefore, the problem of how to accurately distinguish between explosions and earthquakes has already become an important problem of study among seismic activities in mining areas. Nearby, small explosions are relatively easy to distinguish, because the P wave and S wave amplitude ratios and the S wave periods are much different from earthquakes on the seismic record. The identification of far-off nuclear explosions has already become an independent area of study with a great amount of work being done by others outside the country<sup>1</sup>. This paper will primarily discuss the statistical differences between medium distance (100-500 km), medium strength ( $2.5 < M_L < 4.5$ ) explosion and earthquake records, and offer methods of distinguishing explosions based on these differences.

Records of 15 comparatively large industrial explosions recorded since 1969 from China's Xinan, Shanxi, and Beijing (Peking) Seismic Observatories are used in this paper. Each station was equipped with Wiechert vertical component seismograph recording the periods from  $T = 0.05$  s to 1.0 s.

\* Acta Geophysica Sinica, Vol. 18, No. 3 p. 208-216, July, 1975.

## II. Statistical differences between explosion and earthquake records

Sometimes the distinctive features of an explosion are very clear on a seismogram, with no need for a careful examination to conclude that the event is an explosion. Sometimes an explosion has very few differences from an earthquake record and is almost impossible to discern as an explosion. This clearly shows that the differences between explosion and earthquake records have largely statistical variations. Based on the results from large amounts of explosion data, we shall now develop in the discussion the differences between two types.

### 1. The relationship between $t_{\bar{P}-P_n}$ and $t_{\bar{S}-\bar{P}}$

Assuming that the earth's crustal thickness,  $H$ , is 40 km, then the travel times for  $\bar{P}$  and  $P_n$  waves are:

$$t_{\bar{P}} = \frac{1}{v_1} \sqrt{\Delta^2 + h^2}$$
$$t_{P_n} = \frac{\Delta}{v_2} + \frac{2H - h}{v_1} \sqrt{1 - (v_1/v_2)^2}$$

Because explosions are set off at the earth's surface ( $h = 0$ ), and the depth for most earthquakes is  $h = 15-30$  km, the propagation paths of the seismic waves will not be the same, so the relationship between  $t_{\bar{P}-P_n}$  and  $t_{\bar{S}-\bar{P}}$  will also be different. Figure 1 shows the result for a number of explosions and earthquakes. From this figure it can be seen that whether the event is an explosion or an earthquake,  $t_{\bar{P}-P_n}$  and  $t_{\bar{S}-\bar{P}}$  show a linear recursive relationship resembling a binary normal distributed random variation.

To obtain the straight line equation and its parameters, we have for the explosions:

$$t_{\bar{P}-P_n} = a' + b t_{\bar{S}-\bar{P}}$$

where

$$a' = 7.62, b = 0.305, \sigma = 0.478, n = 29.$$

For the earthquake straight line and its parameters we have:

$$t_{\bar{P}-P_n} = \hat{a}' + \hat{b} t_{\bar{S}-\bar{P}} ,$$

$$\hat{a}' = 4.56, \hat{b} = 0.304, \hat{\sigma} = 1.09, \hat{\sigma}_x = 6.71, n = 41,$$

$$\bar{t}_{\bar{S}-\bar{P}} = \frac{1}{n} \sum_{i=1}^n t_{\bar{S}-\bar{P}}^{(i)} = 33.4 .$$

These two straight line equations have clear differences: the points for the explosions lie comparatively close to the straight line, while the data points for the earthquakes have more scatter, and the two lines are separated by about 3 seconds [along the y-axis]. Now using the assumption of a normal distribution (about the lines) in the investigative method<sup>2</sup>, we form n-2 independent equations for t:

$$T_a = \sqrt{n-2} \frac{\hat{a} - a}{\hat{\sigma}} \qquad \hat{a} = \hat{a}' + \hat{b} t_{\bar{S}-\bar{P}}$$

$$T_b = \sqrt{n-2} \frac{\hat{b} - b}{\hat{\sigma}} \hat{\sigma}_x \qquad a = a' + b t_{\bar{S}-\bar{P}} .$$

Using a, b for explosions and  $\hat{a}, \hat{b}$  for earthquakes, we obtain

$$T_a = 17.0$$

$$T_b = 0.038$$

It appears evident from the distribution of t that, using the parameters a and b to examine the two straight lines as a single probability distribution gives

$$P(|t| \geq T_a) = 0$$

$$P(|t| \geq T_b) = 1.0$$

From this it can be seen that the differences between the two straight lines ap-

pear primarily in parameter  $a$ . Because the relationship between  $t_{\bar{P}-P_n}$  and  $t_{\bar{S}-\bar{P}}$  depends primarily on the crustal structure and the focal depth,  $h$ , and the influence of other factors is small, the parameter  $a$  is a basis for distinguishing explosions.

## 2. The relationship between $M_L$ and $M_S$

The relationship between the near-earthquake magnitude,  $M_L$ , and the surface wave magnitude,  $M_S$ , used in China is

$$M_S = 1.13 M_L - 1.08 \quad .$$

Gu Dengbao and Li Wongte's results give

$$M_S = 1.27 (M_L - 1) - 0.016 M_L^2 \quad .$$

These equations clearly show that the local magnitude  $M_L$  of earthquakes is larger than the surface wave magnitude  $M_S$ . However, this is not the case with explosions. Using a May, 1971, explosion as an example, the results of Yunnan Province's Jaotong and Kunming Observatories are ( $M_S$  determined from Jishi [Basic] seismograph,  $M_L$  determined from Wiechert seismograph):

$$\text{Jaotong:} \quad M_S - M_L = 4.7 - 3.8 = 0.9$$

$$\text{Kunming:} \quad M_S - M_L = 4.9 - 3.7 = 1.2$$

$M_S$  is clearly larger than  $M_L$  for explosions, exactly the opposite of what was found for earthquakes, so the quantity  $M_S - M_L$  is one of the differences between the two.

There has already been a large amount of work done outside of China on the use of a similar relationship between the body wave magnitude,  $m$ , and the surface wave magnitude,  $M_S$ , to detect underground nuclear explosions<sup>1,3</sup>.

## 3. The $S_V/S_H$ ratio

If an explosion is detonated in an infinite uniform space, then only longitudinal waves,  $P$ , will be produced. But actual explosion records show not

only P waves, but also S waves. This is because actual explosions are set off in a non-uniform half-space. Based on the symmetry of an explosion, however, the  $S_H$  portion of the S wave should be very small. Starting out from this consideration, the S waves for three explosion events were examined, and the ratios  $S_H/S_V$  were calculated. The results are shown below:

Station	$S_H/S_V$
Xichang	0.19
Mabian	0.05
Tangdan	0.06
Panzhihua	0.28
Quinshui	0.75
Huoxian	0.54
Puxian	0.03

These stations were distributed in different directions around the explosion. For each station,  $S_H$  is less than  $S_V$ , and in most cases it is much less. The average of the values from the seven stations is  $S_H/S_V = 0.27$ .

Below we give a simple analysis, following the method of M. Bath<sup>4</sup>. If we have a displacement  $\bar{U} = \nabla \phi + \nabla \times \bar{A}$  in free space, then  $\phi$  and  $\bar{A}$  will separately satisfy the wave equations:

$$\frac{\partial^2 \phi}{\partial t^2} = a^2 \nabla^2 \phi, \quad \frac{\partial^2 \bar{A}}{\partial t^2} = b^2 \nabla^2 \bar{A}.$$

Under normal conditions, an explosion shows at least cylindrical symmetry, so that in cylindrical co-ordinates:

$$\frac{\partial A_r}{\partial \psi} = \frac{\partial A_z}{\partial \psi} = \frac{\partial \phi}{\partial \psi} = 0.$$

We now write the r,  $\psi$ , and z components of U as u, v, and w below:

$$u = \frac{\partial \phi}{\partial r} - \frac{\partial A_z}{\partial z}$$

$$v = \frac{\partial A_r}{\partial z} - \frac{\partial A_z}{\partial r}$$

$$w = \frac{\partial \phi}{\partial z} + \frac{1}{r} \frac{\partial}{\partial r} (r A_\psi)$$

The above equation shows that in the r-z plane only  $\phi$  and A are involved in the components of motion; these are equivalent to the P and S waves. In the  $\psi$  direction only  $A_r$  and  $A_z$  are non-zero, corresponding to the  $S_H$  wave. Because of the axial symmetry we can divide the  $S_H$  and  $S_V$  components. We first discuss the  $S_H$  wave:

$$v = \frac{\partial A_r}{\partial z}, \frac{\partial A_z}{\partial r}$$

Because of the axial symmetry we have:

$$\sigma_{r\psi} = 2\mu \left( \frac{1}{r} \frac{\partial u}{\partial \psi} + \frac{\partial v}{\partial r} \right) \Big|_{r=\text{arbitrary}} = 0$$

so

$$\frac{\partial v}{\partial r} = 0$$

and since r is the time of the cylindrical radius of the source,  $v=0$ , therefore  $v(r,z) = 0$ .

From this calculation it can be seen that in cases of axial symmetry no  $S_H$  waves will exist, but actual explosions cannot satisfy the axial or spherical symmetry requirement because of the influence of the structure of the medium. So  $S_H$  waves will appear, but will be much smaller than  $S_V$  waves. This is a clear difference between explosions and earthquakes.

#### 4. The ratio of $A_P/A_S$

The statistical results from most earthquakes shows that the P wave amplitude is much smaller than the S wave amplitude, while the results from many explosions shows that the P wave and S wave amplitudes are more similar, with some records showing a much larger P than S wave amplitude. This difference probably arises because of the two different types of source mechanisms. Lamb<sup>5</sup> was the earliest to calculate the ground motion produced by a concentrated perpendicular force, and in 1914 Sharpe<sup>6</sup> calculated a spherical explosive source in an infinite medium. After this there were many calculations concerning

explosive sources. All of the calculations show from a theoretical standpoint the comparatively large amplitude of the P waves. From the figures [2 and 3] one can see that the  $A_p/A_s$  ratio for earthquakes has small scatter, with the values falling between 0 and 1. For explosions, the scatter in the values of the ratio is larger, with the largest value being 2.8. There are many factors influencing the  $A_p/A_s$  ratio for explosions, the most important factors include the explosive mechanism, the structure of the medium, the structure of the observatory foundation, [seismograph pier,] etc. Because of these factors, a single explosion record at an observatory may have a small  $A_p/A_s$  ratio, but from statistical observations at many stations the ratio for explosions will be much larger than for earthquakes.

#### 5. Average period, T, of the S waves

In general it can be said that for observations at the same distances, the S waves from explosions have a larger period than those from earthquakes. The period of S waves from small, nearby explosion records are about 0.1-0.2 seconds longer than those from earthquake records (see figures 4, 5, and 6). Sometimes on the record of a small, nearby explosion, the P and S waves both exhibit a stable period of vibration [i.e., a steady monochromatic frequency content] (figures 7 and 8) which is never observed for earthquakes.

Explosion records in the range of 100-500 km have other distinctive features. Earthquake records have large changes in period from the P wave to the S wave tail, while the change in the period on explosion records is comparatively small. The explosion records are smooth and sleek in appearance, with smaller high frequency perturbations. Figure 9 is a record of the 1969 Pohai earthquake recorded at Madaoyu station, and figure 10 is a record of a 1970 explosion at the same station. In these two figures it is very easy to see these distinctive features.

According to the results of Nersesov<sup>8</sup>, the primary period of the explosion depends mainly on the charge size, and the distance from the shot is not as important. We have examined the mean S wave period,  $T$ , for a number of explosion and earthquake records. Figure 11 shows the relationship between  $T$  and  $M_L$ . From this figure it can be seen that the period of the S waves from explosions is 0.15 to 0.20 seconds larger than the period for earthquakes.

The basic reason for the longer explosion wave periods is the different mechanism in explosions and earthquakes. For explosions, the expanding force is applied for a very short period of time. According to the experimental and observational results of Rulev<sup>9,10</sup>, earthquake records are composed of P,  $P_L$ , and  $S_L$ , and  $S_L$  waves, with the  $P_L$  and  $S_L$  waves arriving separately from and after the P and S waves in a long period wave train with characteristics of both body and surface waves. In explosion records, however, only P,  $P_L$ , and  $S_L$  waves are present, with none of the comparatively short-period S waves (see figures 9 and 10), so that the S component waves on explosive records have an average period longer than the S component waves on earthquake records.

#### 6. S wave decay time $\tau$

The expanding force during an explosion is in effect for only a very short period of time: on the order of milliseconds for most nuclear explosions, and slightly longer for conventional (industrial) explosions. For earthquake sources, however, at least for earthquakes along linear faults, many people consider them to be caused by the process of sliding along a fault; accordingly, the spreading speed of the break can be calculated<sup>11</sup>, and it is found that small earthquakes take a few seconds. The larger the earthquake, the longer the duration of the source. For example, the 1960 Zhili earthquake lasted over 200 seconds. The source duration is therefore shorter for explosions than for earthquakes, and the larger their magnitudes, the larger the difference. Because

of this, the duration of explosion records is shorter than the duration of earthquake records. In particular, since shear stress is the major source of most earthquakes, the difference in the duration of the S waves is very evident. We define the time for the S wave amplitude to decline from its maximum value to one-half the maximum value as the S wave decay time  $\tau$ . Figure 12 shows the relationship between  $\tau$  and  $M_L$  for explosions and earthquakes. From this figure we can see that  $\tau$  is smaller for explosions than for earthquakes, and that the discrepancy is greater for larger magnitudes.

#### 7. Polarity distribution of primary ground motion

The polarity distribution of the first motion of most structured earthquakes has a comparative regularity in all four quadrants. This is not the case for explosions, since the theoretical first motions for explosions should all be positive. Actually, owing to the complex structure of the medium, the conditions at each detector will be different, so that explosions will also show some negative polarity first motions, but the distribution is not regular. Figure 13 shows the polarity distribution of the first motion for a 1971 explosion. This figure clearly shows that negative primary motions from an explosion are a normal phenomena<sup>1</sup>.

#### 8. Surface waves

Love waves are  $S_H$  component surface waves, and Rayleigh waves are  $S_V$  component surface waves. According to earlier theories, explosions should not produce any Love waves<sup>1</sup>. After a  $M_L = 4.6$  explosion at a certain place in May, 1971, a  $M_L = 5.0$  earthquake occurred in the same area in September, offering a very good opportunity for comparison, as shown in figures 14 and 15. A comparison of the two figures shows:

Explosion: There is almost no Love wave at all, the vertical component Rayleigh wave becomes very large, and the record is generally smooth.

Earthquake: The level of the Love wave grows very large, and there is a lot of high frequency disturbances on the record.

To sum up the above discussion, based on dealing with a large number of explosion events, and summarizing the statistical differences between explosion and earthquake seismograms mentioned above, we have proposed a number of useful methods for distinguishing explosions. In actual practice, one must look at all of the conditions, and use a number of techniques to be successful.

### III. Discussion

Because this paper is based on a review of seismograms from the Wiechert seismograph, comparisons [of the results of this paper] with other types of instruments, especially long-period seismographs, will only have value as a [general] reference. Owing to the bandwidth limitations of the instruments, a study of the spectral differences was not conducted.

## References

1. Seismic methods for monitoring underground explosions, an assessment of the status and outlook, Stockholm International Peace Research Institute, 1969.
2. Fudan University Mathematics Dept., Statistical Methods, Shanghai Scientific Methods Press, 223, 1960 (in Chinese).
3. P.W. Basham, Canadian magnitude of earthquakes and nuclear explosions in south-western North America, Geophys. J. R. Astr. Soc. 17, 1-13, 1969.
4. M. Bath, Mathematical aspects of seismology, Amsterdam, Elsevier, 1968.
5. H. Lamb, On the propagation of tremors over the surface of an elastic solid, Phil. Trans. Roy. Soc. (London) A. 203, 1-42, 1904.
6. J.A. Sharpe, The production of elastic waves by explosion pressures, Geophysics, 7, 144-154, 1942.
7. I. Aboadi, The response of an elastic half-space to the dynamic expansion of an imbedded Aspherical cavity, Bull. Seism. Soc. Amer. 62, 115-127, 1972.
8. I.L. Nersesov, A.B. Nikolaev, K voprosy o zavisimosti preobladaushchich chastot pre vzribach ot velichnii zaryda [On the question of the dependence of the predominant frequency on the charge size of an explosion], (Trudi instituta fiziki zemli [Transactions of the Institute of Earth Physics]), No. 25, (192), 1962 (in Russian.).
9. M.A. Sadovskii, Eksperimentalnaya seismologiya (sbornik stateii) [Experimental Seismology], 65-74, 1971.
10. J. Oliver, M. Major, Leaking modes and  $P_L$  phase, Bull. Seism. Soc. Am. 50, 2, 1960.
11. H. Benioff, Earthquake source mechanism, Science, 143, 1399-1406, 1964.

FIGURE CAPTIONS

- 1 - Relationship between  $t_{\bar{P}-P_n}$  and  $t_{\bar{S}-\bar{P}}$   
 x - axis:  $t_{\bar{S}-\bar{P}}$  (seconds)      y - axis:  $t_{\bar{P}-P_n}$  (seconds)  
 upper line - earthquakes      lower line - explosions
- 2 - Relationship between  $A_P/A_S$  and  $\Delta$  for earthquakes  
 x - axis -  $\Delta$  (km)      y - axis:  $A_P/A_S$
- 3 - same as for 2, except for explosions
- 4 - Dahe station earthquake seismogram  
 $t_{\bar{S}-\bar{P}} = 3.3, M_L = 1.6$
- 5 - Dahe station explosion seismogram  
 $t_{\bar{S}-\bar{P}} = 2.2, M_L = 1.2$
- 6 - Dahe station explosion seismogram  
 $t_{\bar{S}-\bar{P}} = 2.3, M_L = 0.7$
- 7 - Dahe station explosion seismogram  
 $t_{\bar{S}-\bar{P}} = 2.2, M_L = 0.9$
- 8 - Panzihua station explosion seismogram  
 $t_{\bar{S}-\bar{P}} = 0.7, M_L = 1.5$
- 9 - Seismogram of Pohai earthquake of August 21, 1968  
 $M_L = 3.4, t_{\bar{S}-\bar{P}} = 32.0$ , Madayu station record
- 10 - Explosion during 1970  
 $M_L = 3.2, t_{\bar{S}-\bar{P}} = 31.0$ , Madayu station record
- 11 - T, the average period of the S waves  
 x - axis:  $M_L$       y - axis: T (seconds)  
 upper line - explosions      lower line - earthquakes
- 12 - S wave decay time  $\tau$   
 x - axis:  $M_L$       y - axis:  $\tau$  (seconds)  
 upper line - earthquakes      lower line - explosions

FIGURE CAPTIONS, Cont.

13 - Polarity distribution of first motions for an explosion during 1971.

o - seismograph location                      \* - explosion location

+, - polarity of first motion

14 - Chengdu station Jishi (Basic) model seismograph record of an earthquake in September 1971

$M_L = 5.0, \Delta = 496 \text{ km}$

15 - ditto 14 except explosion in May, 1971

$M_L = 4.6, \Delta = 496 \text{ km}$

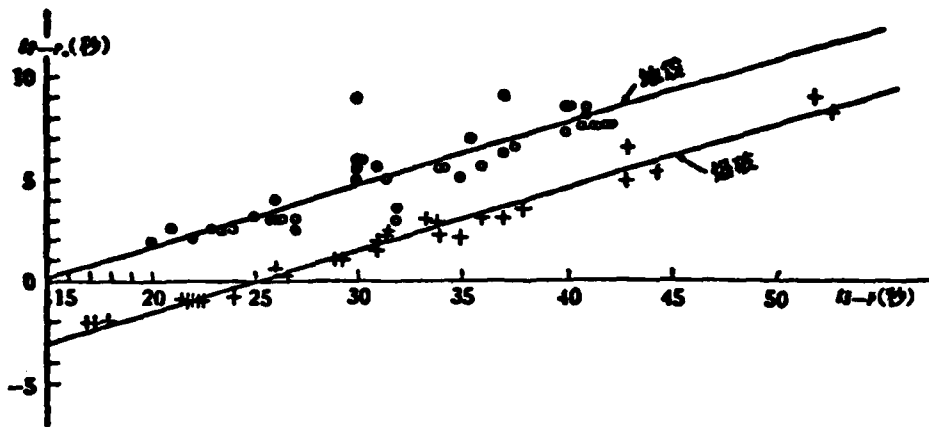


图1  $t_{1-p}$  与  $t_{2-p}$  关系

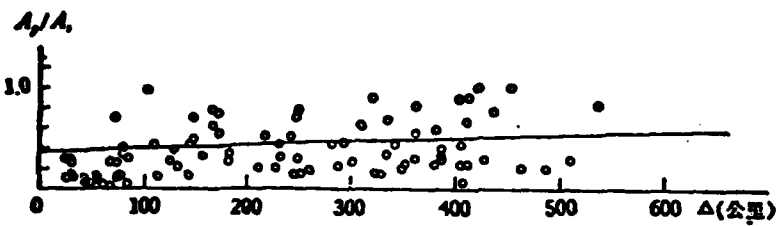


图2 地震的  $A_p/A_s$  与  $\Delta$  关系

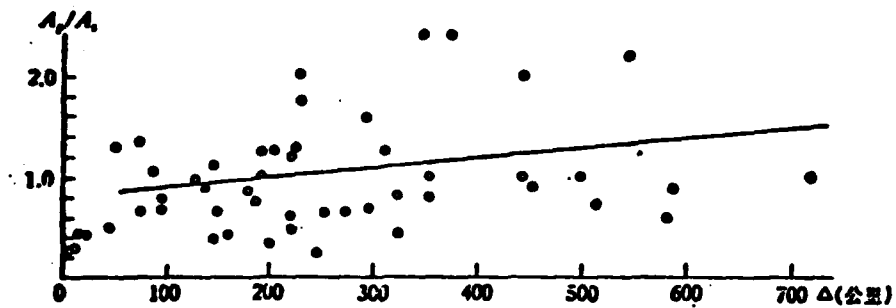


图3 爆炸的  $A_p/A_s$  与  $\Delta$  关系

Figures 1 - 3.

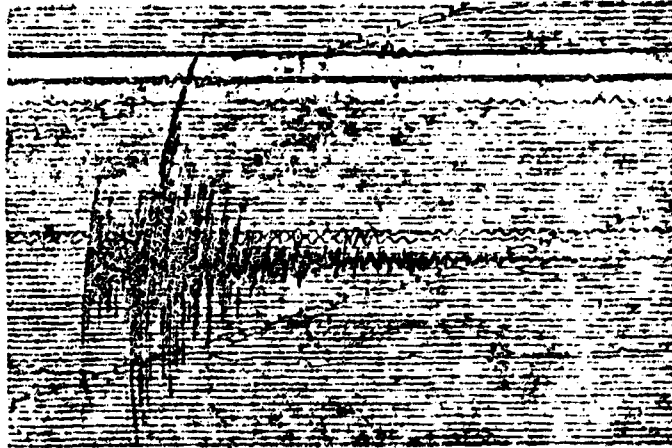


图4 大河台地震记录  
 $ts-p = 3.3, M_L = 1.6.$

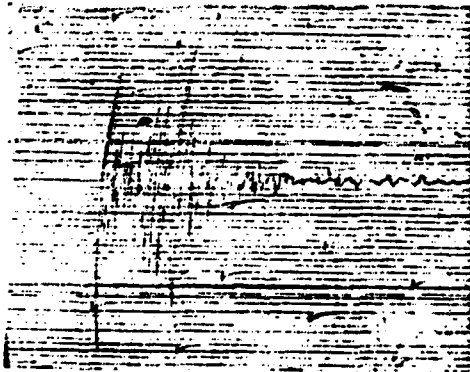


图5 大河台爆破记录  
 $ts-p = 2.2 M_L = 1.2.$

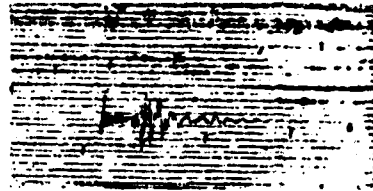


图6 大河台爆破记录  
 $ts-p = 2.3 M_L = 0.7$



图7 大河台爆破记录  
 $ts-p = 2.2 M_L = 0.9.$

Figures 4 - 7.



图 8 翠枝花台爆破记录  
 $t_{S-P} = 0.7$   $M_L = 1.5$ .

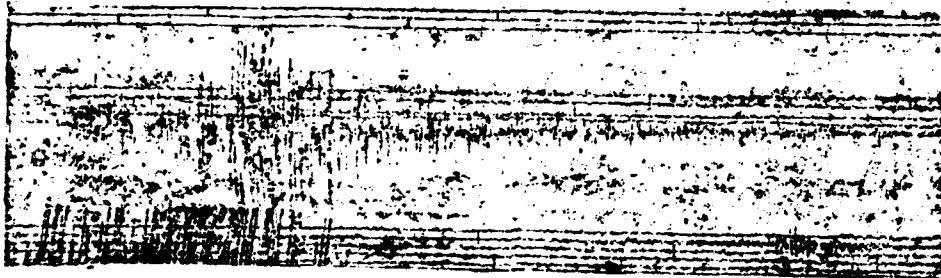


图 9 1968年8月21日渤海地震  
 $M_L = 3.4$ ,  $t_{S-P} = 32.0$ 秒, 马道峪台记录.

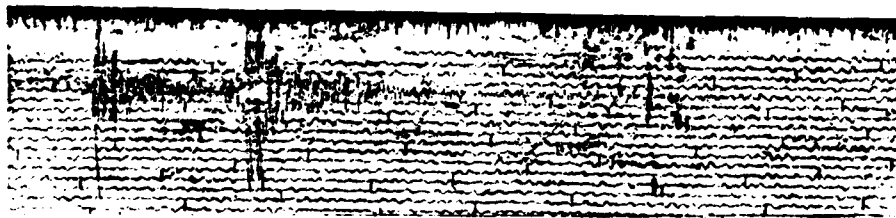


图 10 1970年某地爆破  
 $M_L = 3.2$ ,  $t_{S-P} = 31.0$ , 马道峪台记录.

Figures 8 - 10.

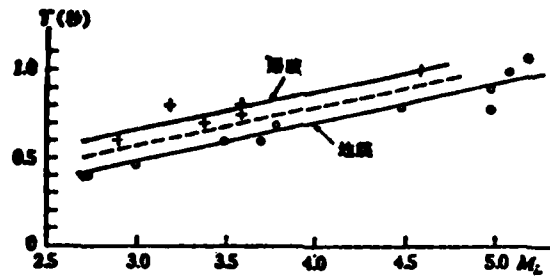


图 11 S波平均周期  $T$

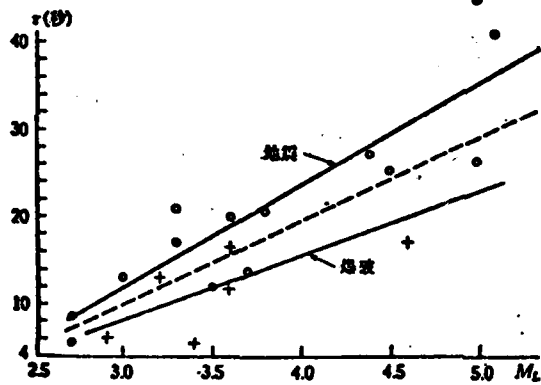


图 12 S波衰减  $\tau$

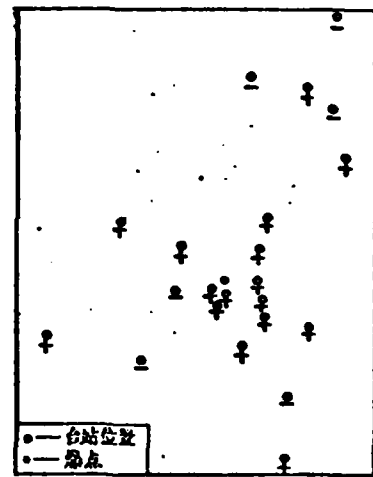


图 13 1971年一次爆破的初动符号分布

Figures 11 - 13.

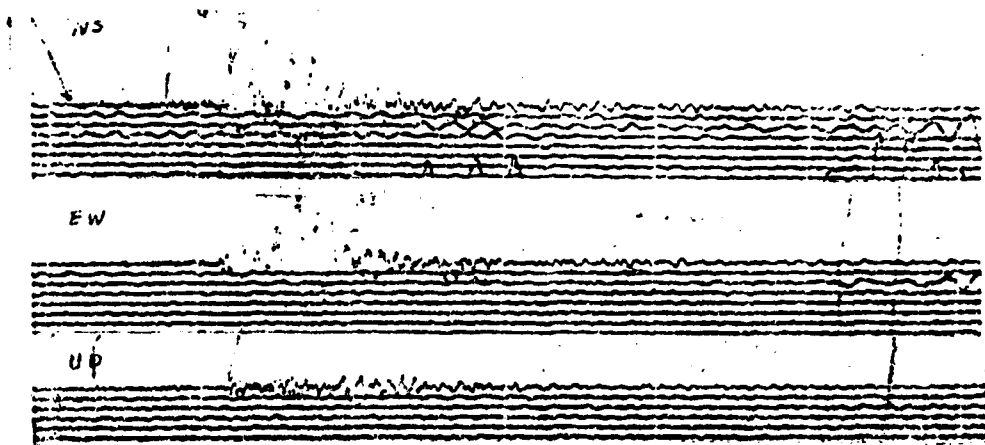


图 14 成都台基式仪记录 1971 年 9 月某地地震  
 $M_L = 5.0$ ,  $\Delta = 496$  公里.

5

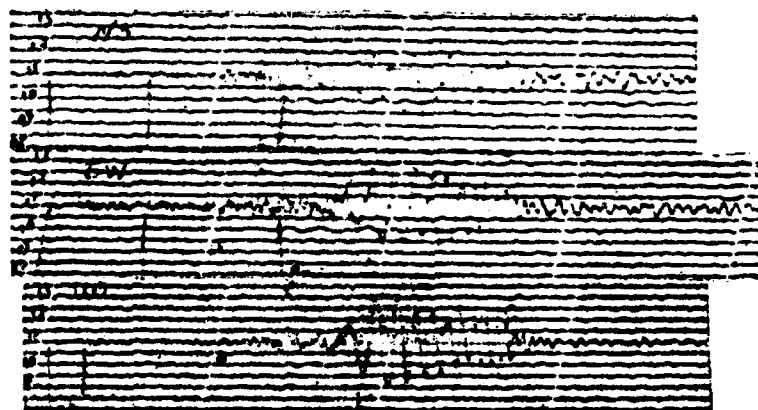


图 15 成都台基式仪记录 1971 年 5 月某地爆破  
 $M_L = 4.6$ ,  $\Delta = 496$  公里.

Figures 14 - 15.

